2020 IEEE International Conference on Robotics and Automation (ICRA)
31 May - 31 August, 2020. Paris, France

Modeling and Analysis of SMA Actuator Embedded in Stretchable Coolant Vascular Pursuing Artificial Muscles

Jaeyeon Jeong[1], Cheol Hoon Park[2], and Ki-Uk Kyung[1*]

Abstract—**This paper proposes a muscle-like SMA (Shape Memory Alloy) actuator with an active cooling system for efficient response. An SMA coil spring is embedded into a stretchable coolant vascular for soften structure of robots. In order to design a flexible, lightweight, and fast-response soft actuator with the SMA coil spring and coolant circulation system, a modeling based approach has been conducted. Analysis of coolant effects has been conducted in aspects of heating speed, cooling speed, and energy consumption based on both theoretical and empirical studies. From thermomechanical and heat transfer model between SMA and coolant, the actuation times in the case of heating and cooling phase have been estimated. From experimental results, Mineral oil is selected as the optimal coolant, and the maximum actuation frequency was measured as 0.5Hz for 40% contraction lifting 1kg.**

I. INTRODUCTION

Recently, flexible robotic system are gaining increasing attention for robot systems in order to overcome disadvantages of conventional mechanism of electrical motor and the gear. Electrical motors can afford high torque, but it needs additional joints and links, which makes the robot heavy and large [1]. To develop a lightweight and compact robotic system, soft actuators that are flexible and can generate a large force with functional materials have been studied [2], [3].

One of the most commonly used materials for soft actuators is a shape memory alloy (SMA). The SMAs have the characteristic of recovering their original shape through a shape memory effect when the temperature goes higher than transition temperature [4]-[8]. Most SMA actuator have been designed as a linear actuator with wire structure since they shows high power density, easy actuation and flexibility [4]. However, the SMA wires have a great disadvantage of having a small strain less than 10%. To overcome the disadvantage of the SMA wire, the SMA coil spring structures were suggested [6], [8]. The SMA coil springs are fabricated by annealing the coiled SMA wires [10], [11], [19], [20]. Since they show much high contraction strain over 50%, which is the same level as the human muscle [8].

One of the main shortcomings of the SMA actuator is the slow response due to the difficulty of gaining both fast heating and cooling speed. Generally, many of the developed SMA-based actuators are operated in ambient air, which offers a fast heating rate but a slow cooling rate as well [4], [11], [12].

Some researches suggest a cooling system with electrical Joule heating to enhance the response speed of the SMA [13]-[16]. Air cooling method with forced air convection is commonly used, but this method still shows a slow cooling rate [13], [14]. Another approach for a fast cooling rate is activating the SMA actuator in water or oil [15]-[17], which shows faster cooling rate than the air case. However, the heating rate and optimization of energy consumption should also be considered.

Recently, some studies that use temperature-controlled water as an actuating source to improve the actuation speed and efficiency [18]-[21]. These actuators contract and extend by flowing the temperature-controlled water through the SMA. Park et al. presented an artificial muscle consisting of a bundle of SMA coil spring and a stretchable tube by applying this mechanism by using valve [19], [20]. Suggested actuator shows an actuating frequency of 1Hz with 50% of contraction strain under a 10kg load condition. However, it needs large reservoirs, thus it is difficult to use as a wearable application.

In this paper, we propose a design process of a muscle-like SMA actuator embedded in stretchable coolant vascular by integrating the SMA coil spring and the stretchable polymer tube with active coolant circulation system. The muscle-like actuator uses an electrical Joule heating to heat up the SMA coil spring. In addition, the active coolant circulation system with a pump and a radiator is integrated with the SMA coil spring for fast cooling rate. In order to select suitable coolant material for the cooling system that shows the fastest actuation speed and the optimized energy consumption, actuation times for various values of thermal properties of the coolants were estimated. Then, the experimental measurement of the actuation times for four coolants were conducted; Water, Mineral oil, Etylene Glycol (EG), and Propylene Glycol (PG). The experimental results show that the actuator using Mineral oil as a coolant can contract and extend with an actuation frequency of 0.5Hz for over 40% contraction strain under a 1kg load condition.

II. MUSCLE-LIKE SMA ACTUATOR EMBEDDED IN STRETCHABLE COOLANT VASCULAR

A. SMA Coil Spring

In order to produce large deformation and high force together, a coil spring shape is applied for a muscle-like SMA actuator with coolant vascular [4], [11], [12]. The relationship between force and displacement of normal coil spring is described in equation (4) when the deformation of the coil spring is small [6].

SMA wire is woven along a steel rod with a diameter of 1.5mm. Then, the SMA fixed on the rod is heated at 350℃ for

*Research supported by the R&D Program (No. 2019R1A2C2006362) of National Research Foundation(NRF), Korea; and also supported by the Translation Research Program for Rehabilitation Robots (NRCTR-EX199006), National Rehabilitation Center, Ministry of Health and Welfare, Korea.

[1]Jaeyeon Jeong and Ki-Uk Kyung are with the Department of Mechanical Engineering, Korea Advanced Institute of Science and Technology(KAIST), 34141, Republic of Korea (e-mail : jjy7583, kyungku) @kaist.ac.kr.

[2]Cheol Hoon Park is with the Depertment of Robotics & Mechatronics, Korea Institute of Machinery and Materials(KIMM), 34103, Republic of Korea (e-mail : parkch@kimm.re.kr).

30 minutes in an oven to memorize its spring shape [10], [11], [19], [20]. Parameters of the SMA coil spring that is used in this paper is shown in TABLE I.

TABLE I

PARAMETER SPECIFICATION OF MUSCLE-LIKE SMA ACTUATOR WITH COOLANT VASCULAR

Parameter	Value
Wire Diameter (d)	0.5mm
Spring Diameter (D)	2.5mm
Number of Coils	55
Transition Temperature (A_f)	40°C
SMA (Nexmetal Co.)	Nitinol (55% Ni, 45% Ti)
SMA Weight	0.8g
Coolant Volume	2.12ml(vascular), 200ml(Reservoir)

Fig. 1 shows the experimental setup for observing the actuation performance of the SMA coil spring. One end of the SMA coil spring was fixed to the load cell, and the other end was fixed to a movable frame. The force was applied to the SMA coil spring by sliding the frame in the direction of extension of the spring, and it was removed by moving the frame in the opposite direction. The relationship between force and displacement was measured at various temperature of 30, 40, 50, 60 and 70°C. The temperature of the SMA coil spring was measured by a thermocouple. Since SMA itself is a resistance, the electrical current was applied to the SMA coil spring to control the temperature.

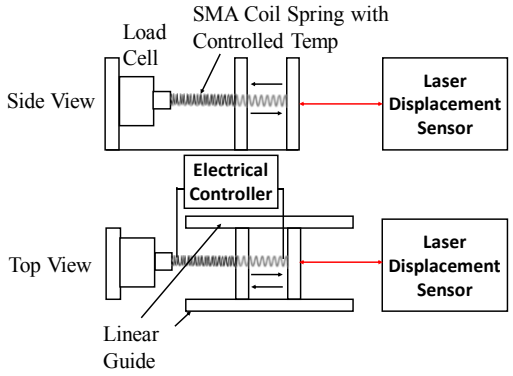

Fig. 1: Experimental Setup for measuring force-displacement relationship of the SMA coil spring.

Fig. 2 shows the relationship between force and displacement at various SMA temperature during one cycle of loading/unloading. Several characteristics of SMA can be observed in the graph. The stiffness of the SMA coil spring increases as the temperature increases. This result implies that the spring constant is higher at high temperature than low temperature. In addition, large range of residual strain is observed after loading/unloading cycle in low temperature since the crystalline arrangement of the SMA was converted from twinned martensite to detwinned martensite [5], [6].

B. *Integration of Active Cooling System and SMA Coil Spring*

An active cooling system by coolant circulation is applied to the proposed actuator with coolant vascular. Fig. 3 shows the schematic of the muscle-like SMA actuator with coolant vascular. A stretchable silicone tube was integrated with the

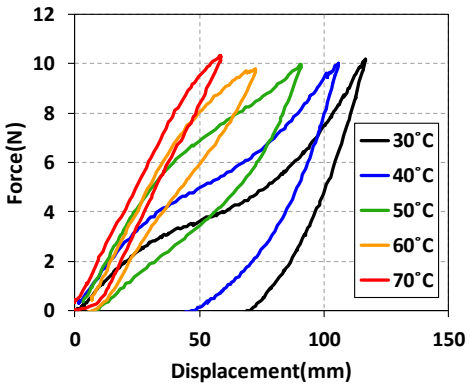

Fig. 2: Force-displacement relationship of the SMA coil spring.

spring [19], [20] for being used as a passage of coolant flow. Since the extension ratio of the SMA coil spring can attain over 200% deformation, the tube should have high stretchability. Both ends of the SMA coil spring and tube were tightly fixed at the connectors, which is used for coolant inlet and outlet. The connector for coolant inlet was connected with a radiator, and the connector for coolant outlet was connected with a pump. A cooling fan was attached to the radiator to cool down the coolant heated by the SMA coil spring.

The stretchable tube was fabricated with Ecoflex 00-30(Smooth on) with a 55mm length and an inner diameter of 7mm. Connectors were fabricated with polycarbonate.

C. *Actuation Mechanism of Muscle-like SMA Actuator Embedded in Stretchable Coolant Vascular*

The actuating mechanism of the muscle-like SMA actuator with coolant vascular is described in the right figure of Fig. 3. The SMA coil spring is surrounded by the stretchable polymer tube and the coolant. As the SMA coil spring is heated, it contracts to recover its original shape. Since the SMA coil spring is a resistance itself, it can be easily heated by electrical current. In cooling phase, the pump that is connected with the actuator and the radiator is turned on. The heated coolant flows to the radiator, and is cooled down with air cooling by the fan. Since the volume of the heated coolant is quite small as mentioned in TABLE I, the volume of the reservoir can be also small.

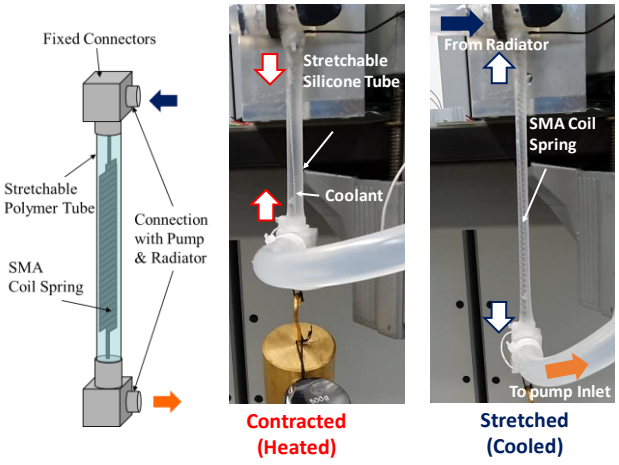

Fig. 3: Muscle-like SMA actuator with coolant vascular.

III. Thermomechanical Model of SMA Coil Spring

Thermomechanical modeling of SMA coil spring can be represented by introducing mechanical model of conventional spring together with constitutive model of SMA. The relationship between the shear stress and shear strain of the SMA coil spring ca be expressed as following equation [5].

$$\tau - \tau_0 = G(\gamma - \gamma_0) + \Omega_\tau(\xi - \xi_0) + \frac{\Theta}{\sqrt{3}}(T - T_0) \quad (1)$$

τ for shear stress, G for shear modulus, γ for the shear strain, Ω_τ for the phase transformation coefficient of SMA, ξ for the volume fraction of martensite phase, Θ for a thermal expansion coefficient of the SMA, and T for temperature of the SMA are considered. Since the deformation occurred by the phase transformation is much larger than by the thermal expansion, the thermal expansion term can be negligible. In addition, phase transformation coefficient can be expressed by a maximum residual strain γ_L and the shear modulus G [5].

$$\Omega_\tau = -\gamma_L G \quad (2)$$

The shear modulus G changes as the temperature of the SMA changes. The shear modulus can be expressed by the function of volume fraction of martensite phase and the shear modulus at fully martensite phase G_M and fully austenite phase G_A , as described in equation (3) [5].

$$G(\xi) = \xi G_M + (1 - \xi)G_A \quad (3)$$

The relationship between force and displacement can be represented by the parameters of the coil spring. The force and displacement can be expressed by the spring parameters [6].

$$\mathrm{F} = \frac{\mathrm{Gd}^4}{8D^3 n}\delta. \qquad \gamma = \frac{\mathrm{d}}{\pi \mathrm{D}^2 \mathrm{n}}\delta \quad (4)$$

F is the force generated by the coil spring, d is the wire diameter, D is the spring diameter, n is the number of coil turns, δ is the displacement of the coil spring, and G is the shear modulus. D, d, and n is design parameters of the coil spring, and G is the properties of material. In the case of SMA, G, the shear modulus, changes as temperature of the SMA changes.

By integrating the equations (1), (2), (3), and (4), the relationship between force and displacement of the SMA coil spring can be expressed in equation (5) [5].

$$C_1(F - F_0) = C_2 G(\xi)(\delta - \delta_0) - C_2 \delta_L G(\xi)(\xi - \xi_0) \quad (5)$$

$$C_1 = \frac{8KD}{\pi d^3},\ C_2 = \frac{d}{n\pi D^2},\ K = \frac{4C-1}{4C-4} + \frac{0.615}{C}(Wahl's\ correction\ factor),\ C = \frac{D}{d}.$$

The volume fraction of martensite phase can be described as a sum of temperature-induced martensite ξ_T, and stress-induced martensite ξ_S [5]. Temperature-induced martensite volume fraction is changed by the phase transformation due to a temperature change, which means the transformation between matrensite and austenite phase. Stress-induced martensite volume fraction is changed due to the phase transformation by the stress, which means the transformation between twinned and detwinned martensite.

IV. Heat Transfer Model

In order to observe the effects of thermal properties of coolant, a heat transfer model that explains the heat transferred from the SMA coil spring to a fluid is considered [15], [18]. Since the heat transfer of coil spring structure is hard to analyze, we selected the diameter of the stretchable tube that is more than twice the spring diameter in order to assume the coil spring geometry as a wire. Then, we applied the heat transfser model of wire geometry [15], [18].

The heat transfer model can be described from the energy conservation equation in specific control volume. The energy conservation equation of the SMA wire and the fluid in control volume can be derived as follows [15], [18], [22]:

$$m_f c_{p,f} \dot{T}_f = q_{SMA \to Fluid} - \dot{m}_f c_{p,f} \Delta T_f \quad (8)$$

$$m_{sma} c_{p,sma} \dot{T_{sma}} = q_{Fluid \to SMA} + \frac{16 I^2 \beta_{sma} c}{(\pi d)^2 \rho_{sma} C_{p,sma}} \quad (9)$$

where T_f temperature of the fluid, $c_{p,f}$ is a specific heat of the fluid, $c_{p,sma}$ is a specific heat of the SMA, and $\dot{m}_f$ is a mass flow of the fluid. The left term of equation (8) is the rate at which heat is stored in the fluid, and $q_{SMA \to Fluid}$ is a heat transfer from the SMA to the fluid. $\dot{m}_f c_{p,f} \Delta T_f$ means a sum of heat transferred into and out of the control volume by the fluid. For simplification, we assumed that the radiation from the fluid to ambient air. The last term of the right side of equation (9) is an electrical energy input to heat up the SMA.

A number of assumptions were considered for constructing the heat transfer model [15], [18]. First assumption is that the wire diameter of the SMA is constant. Poisson's ratio is 0.3 for the SMA, and the normal strain of the SMA wire is very low since the force and displacement of the SMA is dominantly determined by the shear force.

A second assumption is to neglect the radial temperature gradient of SMA wire in the control volume. The Biot number Bi, which means how fast the conduction occurs compared to the convection heat transfer, can be expressed as $\mathrm{Bi} = \frac{\mathrm{hL_c}}{k_{sma}}$. If Bi<<1, the lumped capacitance method can be applied, which means that the temperature of solid at all point in the control volume is constant. The thermal conductivity of the SMA and water are 18W/mK and 0.6W/mK, respectively. Convective heat transfer coefficient h can be expressed by Nusselt number, thermal conductivity, and hydraulic diameter, $\mathrm{h} = \frac{\mathrm{Nuk_f}}{D_h}$. Nu is around 5~10, and the hydraulic diameter is under 10mm in all cases. Therefore, the lumped parameter representation can be justified since the conduction in a radial direction is much larger than the convection.

A third assumption is that the conduction of the SMA wire in a longitudinal direction is negligible. This assumption means that the model is limited to convective heat transfer in the radial direction. Since the cross-section area of SMA is much smaller than the surface area between the coolant and the SMA wire, the conduction is much smaller than convection.

Since the fluid is heated while flowing through the tube, considerations of the temperature change of the fluid is

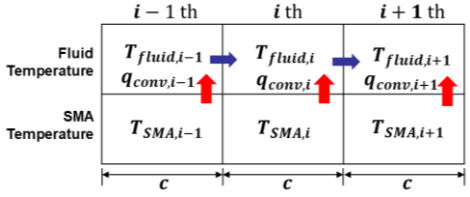

Fig. 4: Temperature profiles and heat transfer of Muscle-like SMA actuator with coolant vascular by segments.

needed. Therefore, the control volume is set to the length of one coil of SMA and the differential equations (8) and (9) are solved numerically. Fig. 4 shows the temperature and heat transfer profiles of the SMA actuator for each segment. The temperature is uniform in each segment. The numerical form of equations (8) and (9) can be expressed as following [18]:

$$\frac{\Delta T_{fluid,i,t}}{\Delta t} = \frac{4\pi D d * h}{\rho_f c_{p,f}((D_{tube}-d)^2 - d^2)}\left(T_{sma,i,t} - T_{fluid,i,t}\right) \quad (10)$$

$$\frac{\Delta T_{sma,i,t}}{\Delta t} = -\frac{4h}{\rho_{sma} C_{p,sma} d}\left(T_{sma,i,t} - T_{fluid,i,t}\right) + \frac{16 I^2 \beta_{sma} c}{(\pi d)^2 \rho_{sma} C_{p,sma}} \quad (11)$$

As time passes, the temperature of the fluid and the SMA is changed due to the heat transfer induced by the temperature difference between the SMA coil spring and the fluid. In heating condition, since there is no flow of fluid, the temperature change occurs independently for each segment. However, as the fluid flows through the next segment, the temperature profiles of the i*th* segment at time t+Δt is changed by the temperature of the i-1*th* segment fluid at time t. The numerical time Δt is described by the length of each segment c and the velocity of the fluid, that is $\Delta t = c/u_f$.

In a heating phase, free convection from the SMA to the fluid occurs since there is no flow of the fluid. Then, Nusselt number of the heating phase can be described by Raleigh number and Prandtl number [15], [21]:

$$\mathrm{Ra} = \frac{g\beta_f (T_{sma} - T_f) D_h^3}{\nu_f \alpha_f}, \qquad \mathrm{Pr} = \frac{\nu_f}{\alpha_f} \left(\nu_f = \frac{\mu_f}{\rho_f}, \alpha_f = \frac{k_f}{\rho_f C_{p,f}}\right) \quad (12)$$

where β_f, ν_f, μ_f, and k_f are the volumetric coefficient of thermal expansion, kinematic viscosity, dynamic viscosity, and thermal conductivity, respectively, of the fluid.

$$\mathrm{Nu} = \left[0.60 + 0.387 \frac{\mathrm{Ra}^{\frac{1}{6}}}{\left[1 + \left(\frac{0.56}{Pr}\right)^{\frac{9}{16}}\right]^{\frac{16}{9}}}\right]^2 \quad (13)$$

$$for\ 10^{-5} \le Ra \le 10^{12}, \qquad \mathrm{h} = \frac{\mathrm{Nuk_f}}{D_h}$$

In a cooling phase, the heat transfer are forced convection. The heat transfer in the cooling phase can be described as follows [15], [22]:

$$\mathrm{h} = \mathrm{k_f} * \frac{0.683 Re^{\frac{1}{2}} Pr^{\frac{1}{3}}}{d} + k_f * \frac{4.15}{Dtube - d} \quad (14)$$

V. Result & Discussion

A. Simulation Results

Several simulations were conducted to select the optimized coolants by observing the effects of coolant materials for efficient actuation. From the thermomechanical model and heat transfer model described in chapter 3 and 4, simulated contraction and extension times for various values of thermal properties were analyzed.

In order to observe the actuation time of the muscle-like SMA actuator with coolant vascular, contraction and extension time were estimated by solving equations (5), (10) and (11) numerically. In the heating phase, the electrical current was applied in a step input of 4A to compare the contraction time in the same energy consumption per time. There is no flow of coolant in this phase. In the cooling phase, no electrical current input is applied to the SMA coil spring.

Several assumptions were made to simulate the dynamic motion of the SMA actuator. First, the force exerted by the stretch of the silicone tube was ignored due to its low elastic modulus, respectively. Second, the actuator was assumed to be in constant load condition that is larger than the final critical stress in the martensite phase of the SMA. Thus, the crystalline arrangement of the SMA coil spring is transferred from the fully detwinned martensite phase to the fully austenite phase. Then, the initial martensite volume fraction in the heating phase is 1, and the initial martensite volume fraction in the cooling phase is 0. In all cases, the force applied to the SMA actuator was assumed to be 10N. The contraction and extension time until the displacement of the SMA coil spring is 45mm for both cases, which is 40% of the initial stretched length, were calculated.

TABLE II

PROPERTIES OF SMA COIL SPRING FOR SIMULATION

Parameters	Symbols	Units	Value
Twinned martensite shear modulus	G_M	GPa	50
Austenite shear modulus	G_A	GPa	100
Martensite start temperature	M_s	°C	55
Martensite finish temperature	M_F	°C	43
Austenite start temperature	A_S	°C	59
Austenite finish temperature	A_F	°C	71
Austenitic constant	C_A	MPa/°C	100
Martensitic constant	C_M	MPa/°C	40
Critical start shear stress	τ_s^{cr}	GPa	0.5
Critical finish shear stress	τ_f^{cr}	GPa	0.9
Density[15]	ρ	kg/m^3	6450
Specific heat[15]	C_p	J/kgK	466 (heat) 260(Cool)
Thermal conductivity[18]	k_f	W/mK	18

TABLE II shows the properties of the SMA coil spring used for the simulation. Temperature values M_s, M_F, A_S, A_F were estimated from the experimental result of the relationship between temperature and displacement. In

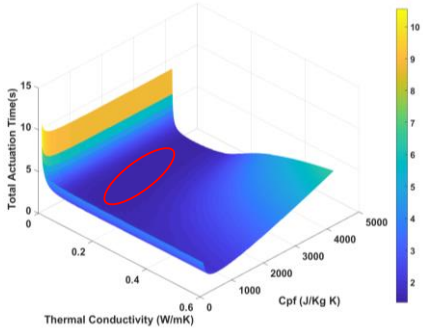

Fig. 5: Simulation results of actuation time of the muscle-like SMA actuator with coolant vascular.

addition, critical stresses τ_s^{cr} and τ_f^{cr} were estimated from the experimental results in the force-displacement relationship in Fig. 2. Density, specific heat and thermal conductivity of the SMA were referred from the previous researches [15], [18].

In the case of the contraction time, as the thermal conductivity and the specific heat increase, the contraction time increases. A large thermal conductivity induces high convective heat transfer coefficient, thus a large heat loss to the coolant can be occurred. In addition, a large specific heat induces a slow temperature increase of the coolant for same heat transfer. Therefore, the temperature difference between the SMA and the coolant becomes large compared to the coolant that has small specific heat as time passes. This result also induces a large heat transfer from the SMA to the coolant.

In the case of the extension time, the flowrate used for calculating the model of the extension time was $5 * 10^{-7} m^3/s$. Long extension time is observed when the specific heat and the thermal conductivity is small, which is opposite in the case of the contraction time. The extension time dramatically increases when the specific heat is under 100J/kgK, and also increases when the thermal conductivity becomes under 0.1W/mK.

The total actuation time was calculated by adding the contraction time and the extension time, as shown in Fig. 5. The shortest actuation time was observed at about 1 second when the thermal conductivity was around 0.07~0.14W/mK and the specific heat was around 1500~2000J/kgK.

B. Experimental Results

In order to select the optimized coolant for the muscle-like SMA actuator with coolant vascular, four coolants that are widely used in the industry were selected; water, Mineral oil, Propylene Glycol(PG), and Ethylene Glycol(EG). The thermal properties of those coolants are shown in TABLE Ⅲ.

TABLE Ⅲ

THERMAL PROPERTIES OF COOLANTS FOR EXPERIMENTS

	Thermal Conductivity k_f (W/mK)	Specific Heat $C_{pf}(J/\text{kg K})$
Water	0.6	4186
EG	0.26	2710
PG	0.147	2500
Mineral Oil	0.136	1670

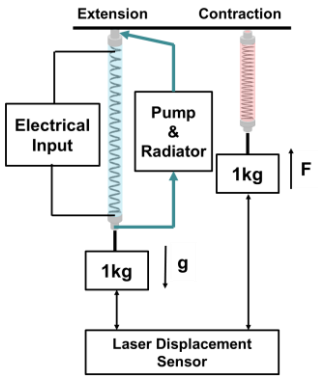

Fig. 7: Experimental setup for measuring actuation times of muscle-like SMA actuator with coolant vascular.

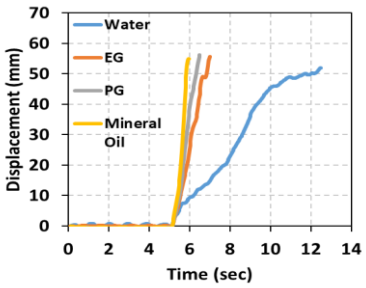

Fig. 8: Experimental results of contraction time of muscle-like SMA actuator with coolant vascular.

Experimental setup for measuring the actuation time is described in Fig. 7. One end of the muscle-like SMA actuator with coolant vascular was fixed on a steel plate, and 1kg mass was attached to the other end of the actuator. In the heating phase, the SMA coil spring was heated by the electrical current input. The step electrical current input of 4A was applied to the SMA coil spring for all cases. In the cooling phase, there is no input to the SMA coil spring and the coolant was circulated by the small pump. In order to observe the effect of the flowrate, the pump was turned on with various power inputs. The displacements of the actuator were measured by the laser displacement sensor.

Fig. 8 shows the measured contraction time of the muscle-like SMA actuator with coolant vascular for various coolant cooling systems. The shortest contraction time was measured as 0.97 seconds when the SMA coil spring was heated in Mineral oil, similar to the simulation result that was estimated as 0.64 seconds. The contraction times were measured as 1.44, 1.96, and 7.6 seconds for PG, EG, and water, respectively. The results show that the contraction time increases as the specific heat and the thermal conductivity increases, which is a similar trend to the simulation results, estimated as 0.73, 0.86, 6.18, respectively with the same order.

In the case of the cooling speed, the extension time decreases as the pump power input increases, which means that the cooling rate becomes fast as the flowrate of the coolant increases. When the same pump input was applied, the shortest extension time was measured as less than 0.5 seconds for water case. EG and Mineral oil cases also show short extension times less than 1 second, but slightly longer than the water case.

The total actuation time can be estimated by adding the extension time and the contraction time. From the

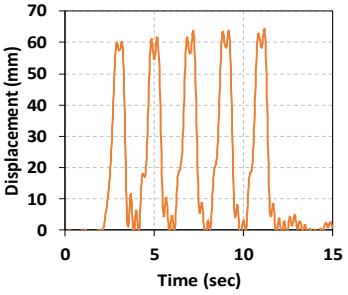

Fig. 9: Cyclic actuation performance of muscle-like SMA actuator with coolant vascular.

experimental results, the Mineral oil cooling case shows the fastest actuation speed in the same system owing to the shortest contraction time and enough fast extension rate. In addition, due to its shortest contraction time, the energy consumption of the actuator is the smallest in the case of Mineral oil cooling case. Cyclic actuation performance of the muscle-like SMA actuator with coolant vascular is described in Fig. 9. The step input of 4A current was applied for the contraction, and the pump input of 1.875W was applied for the extension. Both inputs were applied for 1 seconds, which means the actuation frequency is 0.5 Hz. The maximum contraction strain is measured up to 45%.

VI. CONCLUSION & FUTURE WORK

In order to design a flexible, lightweight, and fast-response soft actuator, a muscle-like SMA (Shape Memory Alloy) actuator with an active cooling system for efficient response is proposed by theoretical and experimental approaches. An SMA coil spring is embedded in a stretchable coolant vascular for soften structure for diverse robot applications, like wearable robots. Analysis of coolant effects has been conducted in aspects of actuation speed and energy efficiency based on both theoretical and empirical studies. From those results, the optimized coolant was selected as Mineral oil, and the maximum actuation frequency was measured as 0.5Hz for 40% contraction under a load of 1kg. The proposed actuator structure shows the possibility of lightweight, enhanced responsive and highly stretchable artificial muscle which is required for wearable applications.

Although the experimental result shows the similar trend to the simulation result, there are still remaining considerations to be investigated beyond the model suggested in this paper for enhanced accuracy of simulation results. For example, the latent heat of the SMA was not included in the heat transfer model due to simplification. In addition, the structural assumption of the heat transfer model might be satisfied in only specified condition, but it was simply assumed in this paper.

As a future work, the improvement of the thermomechanical model and the heat transfer model of the actuator will be studied for a more accurate estimation of the behavior of the proposed actuator, including load-changing condition. In addition, we will improve the performances of the proposed actuator and minimize the size and mass of the actuator in order to use as a wearable application.

REFERENCES

[1] A. J. Veale and S. Q. Xie. Towards compliant and wearable robotic orthoses: A review of current and emerging actuator technologies. Medical Engineering & Physics. 38(4):317-325, 2016.

[2] C. Lee, M. Kim, Y. J. Kim, N. Hong, S. Ryu, H. J. Kim, and S. Kim. Soft robot review. *International Journal of Control, Automation and Systems*. 15(1): 3-15, 2017.

[3] A. Miriyev, K. Stack and H. Lipson. Soft materials for soft actuators. *Nature Communications*. 8:596, pp. 1-7, 2017.

[4] J. M. Jani, M. Leary, A. Subic and M. A. Gibson. A review of shape memory alloy research, applications and opportunities. *Materials & Design*. 56, pp. 1078-1113, 2013.

[5] L. Brinson. One-dimensional constitutive behavior of shape memory alloy: Thermomechanical derivation with non-constant material functions and redefined martensite internal variable. *Journal of Intelligent Material Systems and structures*. 4(2): 229-242, 1993.

[6] S. M. An, J. Ryu, M. Cho, K. J. Cho. Engineering design framework for a shape memory alloy coil spring actuator using a static two-state model. *Smart Materials and Structures*. 21, 2012.

[7] C. Liang, C. A. Rogers. One-dimensional thermomechanical constitutive relations for shape memory materials. *Journal of Intelligent Material Systems and Structures*. 8(4): 285-302, 1997.

[8] H. Tobushi, K. Tanaka. Deformation of a shape memory alloy helical spring : analysis based on stress-strain-temperature relation. *JSME International Journal*, 34(1): 83-89, 1991.

[9] I. W. Hunter, S. Lafontaine. A comparison of muscle with artificial actuators. *In proceedings of Technical Digest IEEE Solid-State Sensor and Actuator Workshop*. 1992.

[10] S. J. Yates and A. L. kalamkarov. Experimental study of helical shape memory alloy actuators : Effect of design and operating parameters on thermal transient and stroke. *Metals*, 3(1): 123-149 2013.

[11] S. J. Park and C. H. Park. Suit-type wearable robot powered by shape memory alloy based fabric muscle. *Scientific Reports* 9:9157, 2019.

[12] A. Villoslada, A. Flores, D. Copaci, D. Blanco and L. Moreno. High-displacement flexible shape memory alloy actuator for soft wearable robots. *Robotics and Autonomous Systems*. 73, pp. 91-101, 2015.

[13] J. Hope and A. McDaid. Development of wearable wrist and forearm exoskeleton with shape memory alloy actuators. *Journal of Intelligent & Robotic Systems*, 86(4): 397-417, 2017.

[14] Y. Tadesse, N. Thayer and S. Priya. Tailaring the response time of shape memory alloy wires through active cooling and pre-stress. *Journal of Intelligent Material Systems and Structures*. 21(1):19-40, 2009.

[15] S. S. Cheng, Y. Kim and J. P. Desai. Modeling and characterization of shape memory alloy springs with water cooling strategy in a neurosurgical robot. *Journal of Intelligent Material Systems and Structures*. 28(16):2167-2183, 2017.

[16] A. M. Nizamani, J. Daudpoto and M. A. Nizamani. *Shape Memory Alloys – Fundamentals and Applications*. Rijeka. Croatia: InTech, 2017.

[17] A. Pathak, D. Bre and J. Luntz. Transformation strain based method for characterization of convective heat transfer from shape memory alloy wires. *Smart Materials and Structures*. 19(3), 2010.

[18] J. D. Ertel and S. A. Mascaro. Dynamic thermomechanical modeling of a wet shape memory alloy actuator. *Journal of Dynamic Systems, Measurement, and Control*. 132(5), 051006, 2010.

[19] C. H. Park and Y. S. Son. SMA spring-based artificial muscle actuated by hot and cool water using faucet-like valve. *In Proceedings of SPIE 10164 Active and Passive Smart Structures and Integrated Systems*, 2017.

[20] C. H. Park, K. J. Choi and Y. S. Son. Shape memory alloy-based spring bundle actuator controlled by water temperature. *IEEE/ASME Transactions on Mechatronics*. 24(4):1798-1807, 2019.

[21] S.W. Churchill and H. H. Chu. Correlating equations for laminar and turbulent free convection from a horizontal cylinder. *International Journal of Heat and mass transfer*. 18(9):1049-1053, 1975.

[22] F. P. Incropera, D. P. Dewitt, T. L. Bergman and A. S. Lavine. *Principles of heat and mass transfer*, 7th edition, Wiley, 2013.